

# Ultra-Wide-Band Microstrip Patch Antenna Design for Breast Cancer Detection

Adel AlOmairi<sup>ORCID</sup>, Doğu Çağdaş Atilla<sup>ORCID</sup>

Department of Electrical and Computer Engineering, Altınbaş University, İstanbul, Turkey

**Cite this article as:** A. AlOmairi, and D. Ç. Atilla, "Ultra-wide-band microstrip patch antenna design for breast cancer detection," *Electrica*, 22(1), 41-51, Jan. 2022.

## ABSTRACT

In this paper, a novel design for an ultra-wide-band (UWB) microstrip antenna with enhanced bandwidth for early detection of breast cancer has been proposed. It has been designed using CST software, which is a 3D analysis software package for electromagnetic components and systems design, analysis, and optimization. FR-4 has been used as a substrate, with dimensions of 60 × 70 mm, having a circular patch with a defected ground structure to reach the desired outcomes. The antenna has a peak gain of 4.431 dBi and works between 1.6 GHz and 10 GHz, which gives a bandwidth of 8.4 GHz with an average of -15 dB. The result of the simulation is presented in terms of radiation pattern, bandwidth, and return loss, and the validation of the proposed work is presented by the gain and the efficiency. A breast phantom model has been designed containing a tumor placed in a specific location, This, when combined with the kinetics of contrast medium propagation in various tissues, may effectively simulate normal breast tissue. The cancerous tumor is detected using specific absorption rate (SAR) analysis. The SAR is the rate of energy absorption in a tissue and is measured in W/kg. The SAR results are a maximum at the coordinates (1.085, 9.47273, 32.25), close to the actual location of the tumor at (0, 10, 40) The results display the ability to detect the tumor inside the breast and to reveal its location with high accuracy, and the antenna radiation meet the SAR standards.

**Index Terms**—Breast cancer detection, CST, ultra-wide-band antenna, wearable devices.

## I. INTRODUCTION

Cancer is one of the deadliest diseases, especially when it becomes malignant and invades the body, spreading to the other organs. It results from the abnormal growth process of cells and is hard to detect even with modern technology. One of the most common types of cancer worldwide is breast cancer, which claims the lives of many women. Therefore, while it is imperative to address this situation and to find a solution by developing a cure, it is even more important to develop methods to detect its presence in the body. Years of research have proved that the most important element in curing cancer is detection in the early stages, before it becomes uncontrollable and spreads to more organs. Many techniques have been proposed, like mammography [1], MRI [2], and ultrasound detection [3]. These technologies are of limited value in detecting cancer on an early stage, mostly due to poor contrast. Therefore, by the time a cancer is detected, the probability of cure is reduced.

The antenna is a device that transmits and receives signals in the form of electromagnetic waves [4]. It has been implemented in the medical field in general applications and more specifically, in cancer. It has been used for diagnosis and treatment, while sometimes only to transmit information. Radio frequency identification (RFID) is used in monitoring systems and medical implants, and in microwave imaging. Thus, antennas can be used for communication and/or as a treatment device.

Several techniques have been used to detect cancer, such as microwave imaging [5] and radar-based microwave tomography [4-7].

Malignant breast tumors are detected using ultra-wide-band microwave [8]. The UWB can be achieved by several antennas such as a microstrip in [9] with a bandwidth ranging from 8.1 to 12.8 GHz, having a defected ground structure. A simple composition can be made to produce an antenna array having a bandwidth ranging from 300 MHz to 4.15 GHz [10]. The metamaterial (MTM) technique is proposed in [11] in order to achieve better performance in terms of efficiency and gain, in a UWB planner antenna for systems of wireless communication.

### Corresponding Author:

Adel AlOmairi

### E-mail:

adel.alomairi@ogr.altinbas.edu.tr

**Received:** May 22, 2021

**Revised:** September 24, 2021

**Accepted:** September 30, 2021

**Available Online Date:** November 17, 2021

**DOI:** 10.5152/electrica.2021.21053



Content of this journal is licensed under a Creative Commons Attribution-NonCommercial 4.0 International License.

In [a], a detailed assessment of the idea, theory, and applications of compound right/left-handed transmission lines (CRLH-TLs) in antenna system designs has been presented. For all instances based on CRLH MTM-TLs, assessments are conducted based on physical dimensions, frequency bandwidth, materials, gain, radiation efficiency, and radiation characteristics. Because of the usage of MTM, structural complexity is reduced. The MTM antennas outperform conventional antennas thanks to a more cost-effective production process. Mohammad Alibakhshikenari and colleagues used the CST Microwave Studio to conduct a feasibility analysis on a novel design for a super-wide impedance planar antenna based on a  $2 \times 2$  microstrip patch antenna (MPA) [b]. The suggested antenna construction overcomes the limited bandwidth of the current microstrip patch designs. The antenna is suitable for microwave and millimeter-wave systems such as UWB, RFID, massive MIMO for 5G, and radar systems. In [c], Mohammad Alibakhshikenari offers a thorough systematic and theoretical investigation of different mutual-coupling suppression (decoupling) strategies, with a particular emphasis on metamaterial and metasurface (MTS) methodologies. It is demonstrated that mutual-coupling reduction solutions prompted by MTM and MTS theories can provide an increased level of isolation between neighboring radiating elements using easily realistic and cost-effective decoupling structures, with negligible impact on the array's properties such as bandwidth, gain, radiation efficiency, and physical footprint using SAR for microwave imaging [12-14].

It is known that the frequency of the microwave band increases in the human body. Therefore, to ensure the safety of the human body and to determine whether it is affected by the radio waves, SAR is usually used in wireless devices. The SAR can be used for isolation improvement as a technique of coupling in a microstrip array antenna [15]. We need flexible antennas with a compact size, a low impact on the human body, and a small SAR; for example, for communication outside the body, patch antenna is used due to its relatively small size, simple design, and high gain [5-7], [15-24] characteristics.

For medical applications, specifically in imaging, diagnosis, and treatment, microstrip antennas are widely used [25]. Moreover, a microstrip is easy to install in the human body due to its flexibility, and the concept of wearability is used in this domain, to ensure flexibility [26].

A wearable microstrip patch antenna is designed, which is known for its small size, low cost of fabrication, and low energy consumption. The mathematical approach, a basic circular antenna design, and the proposed antenna will be discussed in Section II of this paper. The results of the simulations can be seen in Section III. In Section IV, the breast phantom model is shown additionally, and the proposed method of detection can be seen in Section V. Finally, Section VI presents the discussion and conclusion.

## II. METHODOLOGY

### A. Mathematical Approach

This section deals with the design formulas for the basic microstrip patch antenna [27]. These formulas have been used to construct a mathematical model, which forms the fundamental design. This is the initial step in achieving the final design and then adjusting it to meet the required results.

### 1) Antenna Design Procedure

For finding the width [25]:

$$w = \frac{C}{2f_o \sqrt{\frac{\epsilon_r + 1}{2}}} \quad (1)$$

Based on the height, width, and dielectric constant of the substrate, the effective dielectric constant can be found [28]:

$$\epsilon_{eff} = \frac{(\epsilon_r + 1)}{2} + \frac{(\epsilon_r - 1)}{2} \left[ 1 + 12 \frac{h}{W} \right]^{-\frac{1}{2}}. \quad (2)$$

For finding the effective length [25]:

$$L_{eff} = \frac{C}{2f_o \sqrt{\epsilon_{eff}}}. \quad (3)$$

For finding the length extension [28]:

$$\Delta L = 0.412h \frac{(\epsilon_{eff} + 0.3) \left( \frac{W}{h} + 0.264 \right)}{(\epsilon_{eff} - 0.258) \left( \frac{W}{h} + 0.8 \right)}. \quad (4)$$

Then, finally finding the actual length of the patch [28]:

$$L = L_{eff} - 2\Delta L \quad (5)$$

having the following parameters:

$c$  is the speed of light,  $3 \times 10^8$  (m/s)

$f_o$  is the resonance frequency (Hz)

$\epsilon_r$  is the relative permittivity of the dielectric substrate (F/m)

$W$  is the width of the patch (mm)

$h$  is the thickness (mm)

$L$  is the length of the patch (mm).

Based on the formulas of rectangular microstrip antenna, the circular antenna can be obtained. The radius is given by [4]:

$$\text{radius} = \frac{\sqrt{(W+h) \times (L+h)}}{2} \quad (6)$$

where  $W$  is the width,  $L$  is the length, and  $h$  is the thickness. It has been found that multiplying the thickness of the patch by 1.5 gives more accuracy. Thus, the formula will be [4]:

$$\text{radius} = \frac{\sqrt{(W+h \times 1.5) \times (L+h \times 1.5)}}{2}. \quad (7)$$

The radius can also be found by using the resonant frequency ( $f$ ) using [4]:

$$r = \frac{k_{nm} \times c}{2\pi f_r \sqrt{\epsilon_r}} \quad (8)$$

Having  $\epsilon_r$  as relative permittivity,  $k_{nm}$  is  $m$ th zero of the derivatives of the Bessel function of order  $n$ , and  $c$  is the velocity of light in free space.

### B. Designing the Basic Antenna

To begin the detection process, we started with a basic design of a microstrip circular patch antenna with a specific dimension to be placed over the breast. The advantages of using a circular patch over the normal rectangular patch are a better bandwidth [29] and the ability to use the design formula to retrace the frequency at which those dimensions of the antenna will operate.

A  $60 \times 70$  mm circular microstrip patch antenna is designed with the FR-4 substrate with a dielectric property of  $\epsilon_r = 43$ . The design can be seen in Fig. 1, and the measurements are shown in Table I.

### C. Designing the Antenna

A partial ground technique is used to increase the capacitance between the radiating surface and ground to reduce the radiation of the back lobe [30]. The ground plane width is 58.5 mm With two side slots of 2.25 mm, and with a rectangular slot of 1 mm length and 10 mm width, the defected ground ensures wide bandwidth and better gain [31]. Additionally, the feedline has been adjusted to 3.1 to ensure impedance matching with 50 ohms. The substrate dimensions of the proposed design are  $63 \times 72$  mm, keeping the FR-4 as the substrate with thickness of 1.6 mm and copper as the radiating surface with thickness of 0.1 mm. The circular patch has the same radius of 18 mm. However, patch antennas have their own limitations, such as small bandwidth and poor gain. In order to achieve better results, we used different slotting techniques, a slot of 14 mm

width and 0.5 mm length has been made in the center of the patch, which yields better performance and better gain and bandwidth for this design. The design can be seen in Fig. 2. The dimensions are shown in Table II.

## III. THE RESULTS OF THE SIMULATION

### A. Return Loss and Voltage Standing Wave Ratio

The basic design shows a good return loss, as seen in Fig. 3. However the voltage standing wave ratio (VSWR) is above 2 as shown in Fig. 4, which indicates a mismatch that will cause a high reflection of the power. This problem must be solved to obtain better bandwidth. Thus, we should have an original approach to achieve better VSWR performance. The proposed technique is discussed in the next sections.

The return loss S11 can be seen in Fig. 5, which shows an ultra-wide-band that ranges from 1.6 GHz to 10 GHz under -10 dB. The VSWR is less than 2 for the whole range of the band, as shown in Fig. 6.

### B. Radiation Pattern, Gain, and Directivity

The proposed antenna experiences a gain and directivity of 4.431 dBi and 5.197 dBi, respectively, as shown in Fig. 7 and 8, respectively. Fig. 9 shows the radiation gain and efficiency curves. The radiation pattern at 3.664 GHz is shown in Fig. 10.

## IV. BREAST PHANTOM MODEL

In this section, a breast phantom model having 4 mm thickness, seen in Fig. 11, is designed using CST, to simulate the antenna, and the results are observed. In the modeling of the model, proper material has to be chosen, since CST software does not contain those materials in its libraries by default. Therefore, a material definition is provided having the parameters of permittivity, electrical conductance, density, heat capacity, and thermal conductance, listed in Table III, for each layer [32,33]. A tumor is placed at a location having the coordinates of (0, 10, 40) to test our antenna. The tumor has the parameters listed in Table III. Fig. 12 and 13 show the breast phantom along with the tumor.

## V. CANCER DETECTION USING SAR

The SAR is a measurement of the absorption of the electromagnetic energy by human tissues when exposed. It is defined as the power absorbed by tissues per mass, its unit of measure is Watts per

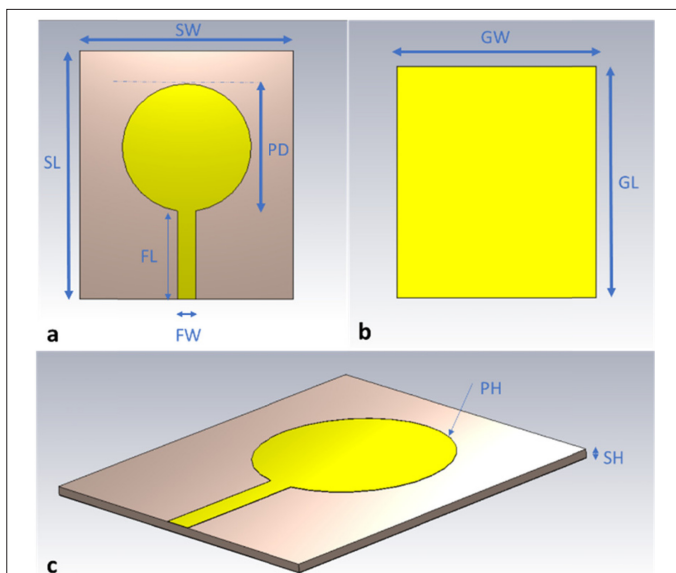
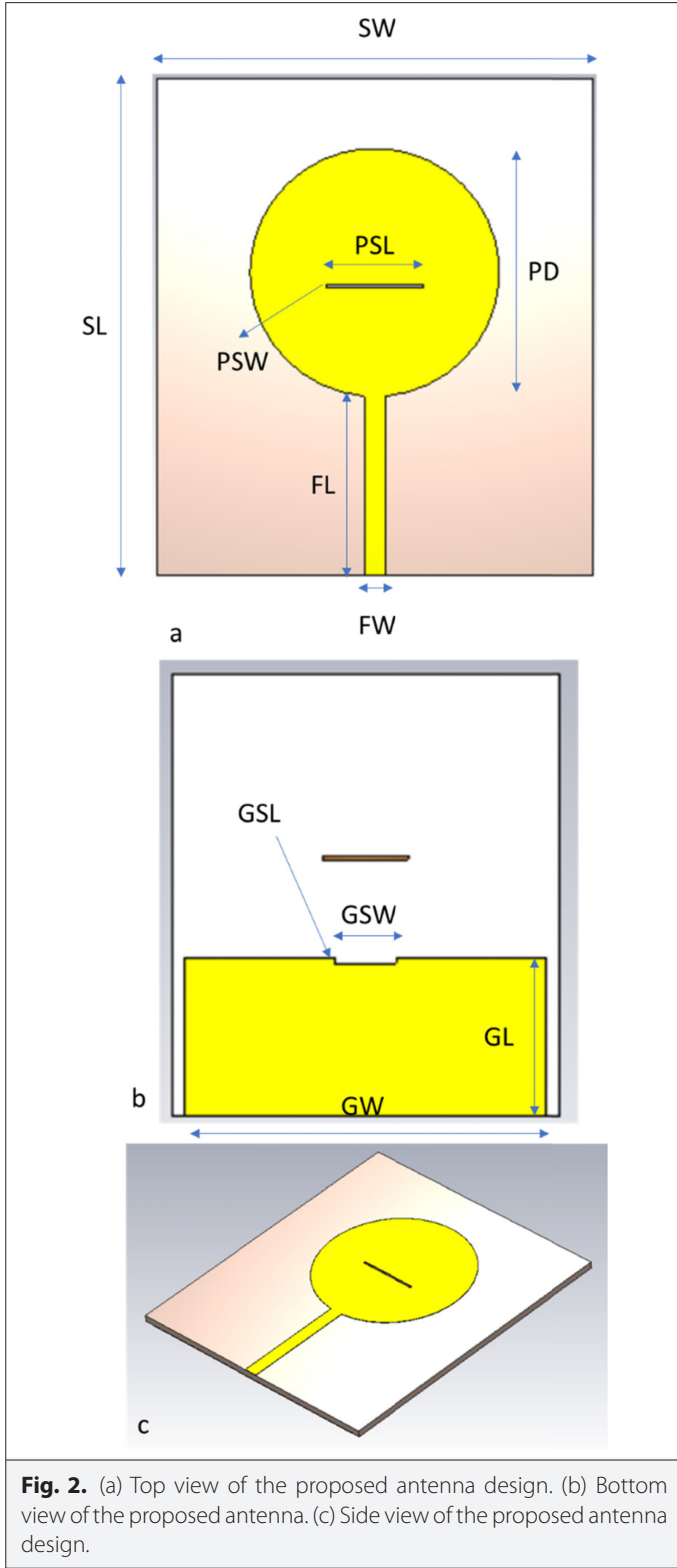


**Fig. 1.** (a) Top view of the circular antenna design. (b) Bottom view of the circular antenna design. (c) Side view of the circular antenna design.

**TABLE I.** CIRCULAR DESIGN DIMENSIONS

Symbol	Dimension (mm)
SW	60
SL	70
FW	5
FL	25
PD	36
SH	1.6
PH	0.1



kilogram. The SAR value can be used for 10 g mass of tissue, the values will be calculated in W/kg at each point in the tissue [33]:

$$SAR_{local}(r, \omega) = \frac{\sigma(r, \omega) |E(r, \omega)|^2}{2\rho(r)} \quad (9)$$

**TABLE II.** PROPOSED ANTENNA DIMENSIONS

Symbol	Dimension (mm)	Description
SW	63	The width of the substrate
SL	72	The length of the substrate
FW	3.1	The width of the feedline
FL	26.5	The length of the feedline
PD	36	The diameter of the patch
SH	1.6	The height of the substrate
PH	0.1	The height of the patch
GW	58.5	The width of the ground
GL	25.7	The length of the ground
GSW	10	The width of the slot of the ground
GSL	1	The length of the slot of the ground
PSW	14	The width of the slot of the patch
PSL	0.5	The length of the slot of the patch

Calculation of the local SAR value can be made using (10). First, a cube having specific mass is found for each point. The power loss density is then integrated over the cube, and the value in total is divided over the mass of the cube. Calculation of the average SAR value can be made using (10):

$$SAR_{average}(r, \omega) = \frac{1}{V} \int \frac{\sigma(r, \omega) |E(r, \omega)|^2}{2\rho(r)} dr \quad (10)$$

Having the  $\sigma(r, \omega)$  material conductivity [S/m], dielectric material density at  $r$  in [kg/m<sup>3</sup>] as  $\rho^i(r)$  – mass,  $E(r, \omega)$  the electric field within the tissue [V/m], and the volume is  $V$  [m<sup>3</sup>]

The breast phantom model is placed (20 mm) away from the antenna, which will radiate toward the phantom, and the response is reflected back to the antenna so that the antenna can receive it, as seen in Fig. 14.

The simulation is made for 10 g of mass tissue at 3.664 GHz having the tumor located at the coordinates (0, 10, 40).

The results of the simulation show a maximum SAR value of 0.69, which satisfies the SAR limitation of 1.6 W/kg, which is considered as hazardous for the human body. Thus, the antenna can be used for biomedical applications because the maximum SAR value is less than 1.6 W/kg. The coordinates where the maximum SAR value occurs are (1.085, 9.47273, 32.25) [mm] where  $x=1.085$ ,  $y=9.47273$ , and  $z=32.25$  as shown in Table IV.

The tumor was located manually at (0, 10, 40) [mm], where  $x=0$ ,  $y=10$ , and  $z=40$  when designing the breast phantom model, which

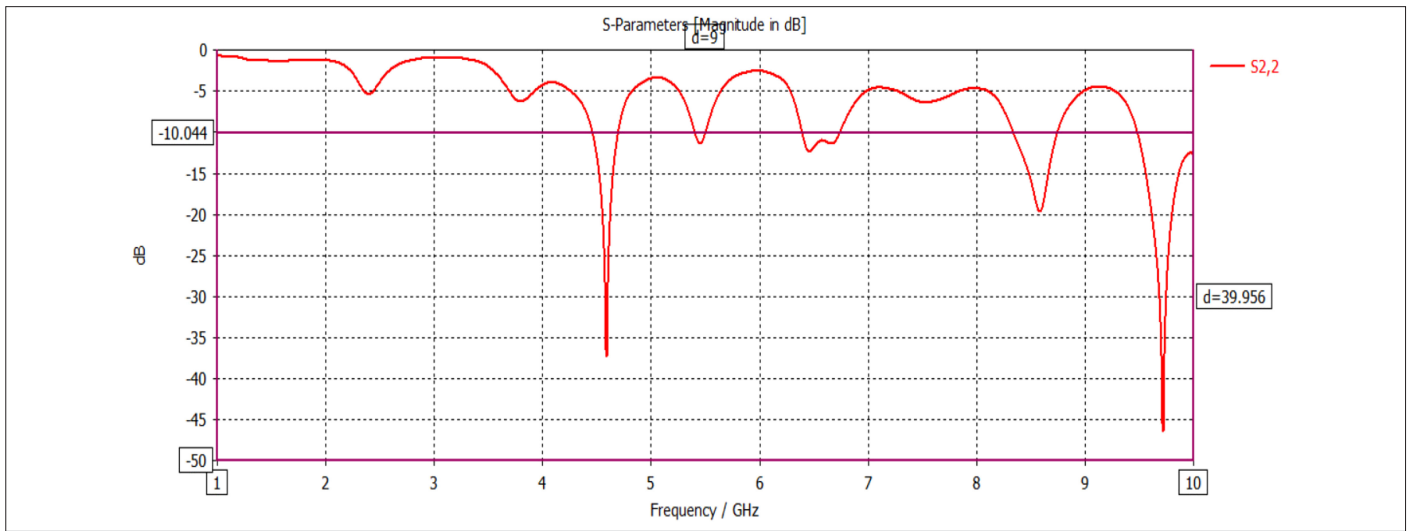


Fig. 3. Return loss results of the basic design.

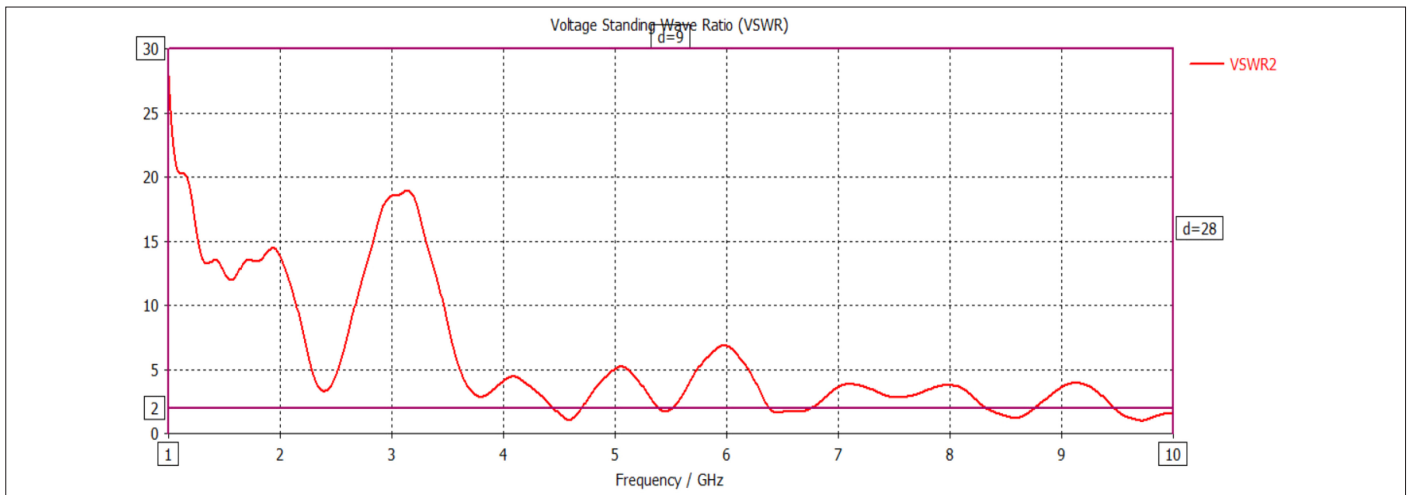


Fig. 4. VSWR results of the basic design.

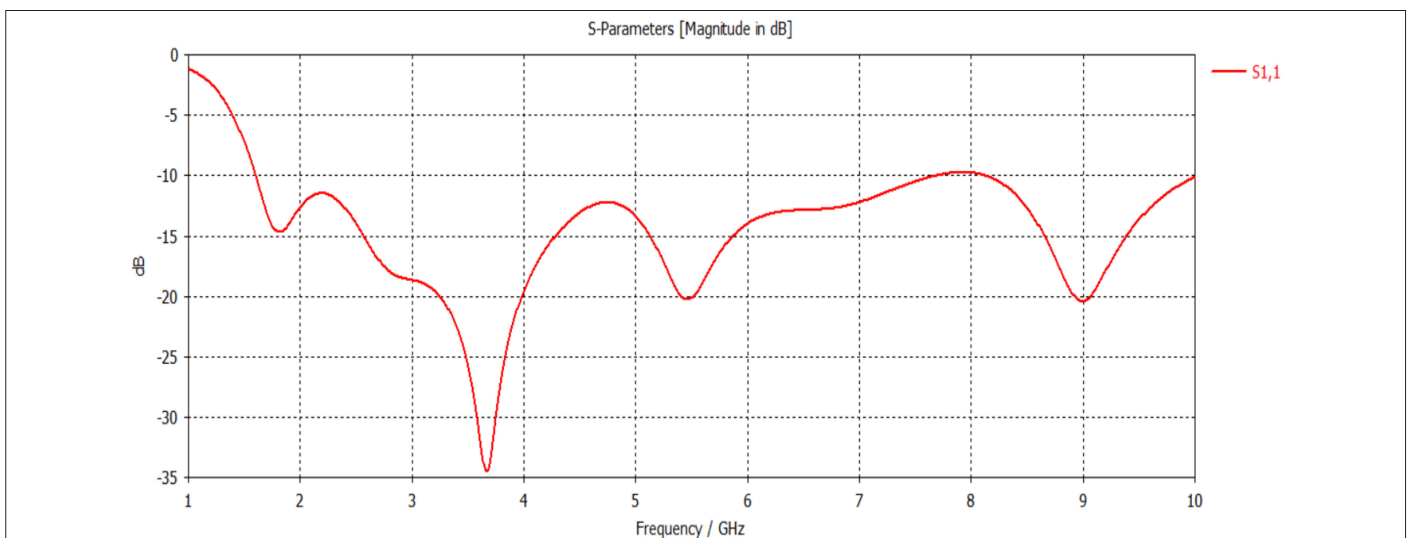


Fig. 5. Return loss of the proposed antenna.

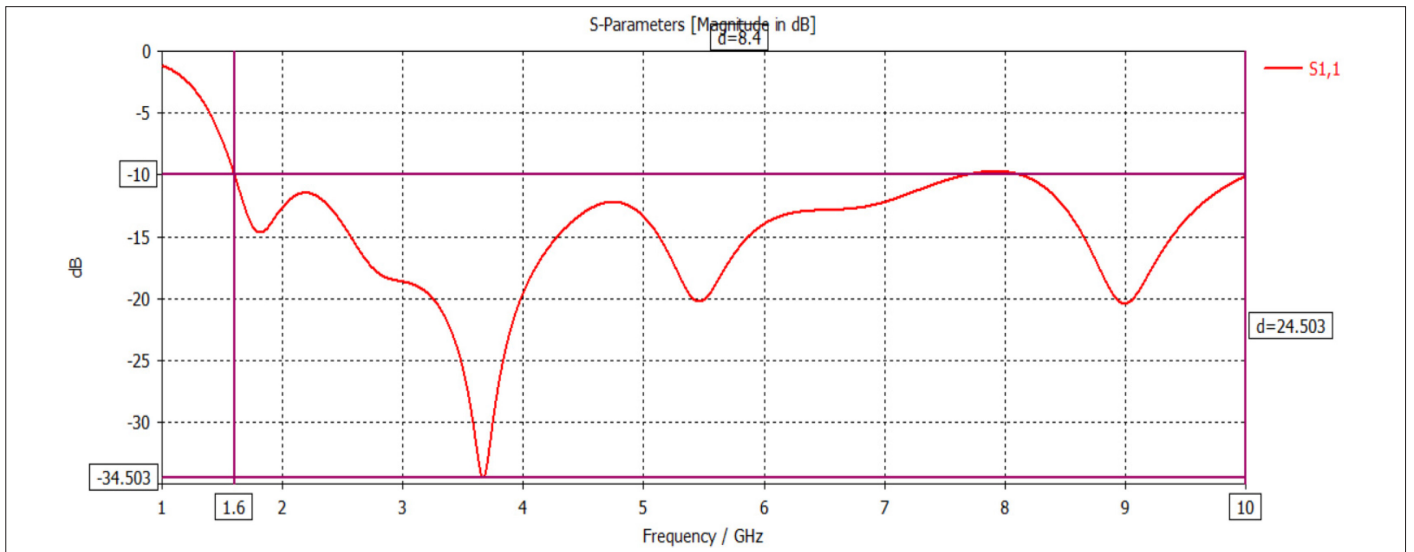


Fig. 6. VSWR of the proposed antenna.

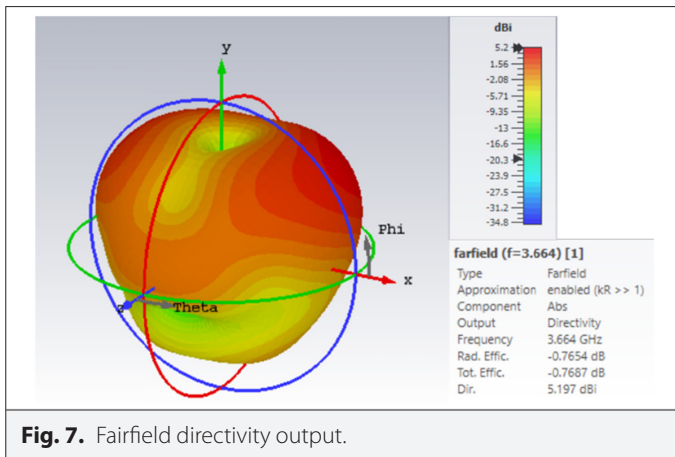


Fig. 7. Farfield directivity output.

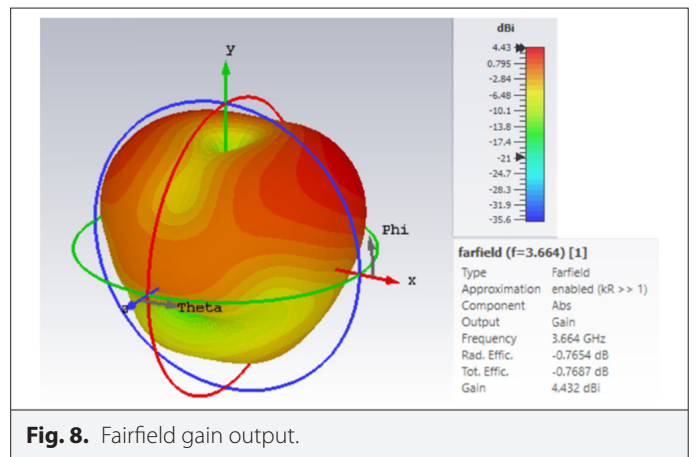


Fig. 8. Farfield gain output.

is considered the real tumor location. After the SAR analysis, the location of the tumor is predicted at (1.085, 9.47273, 32.25) [mm], where  $x=1.085$ ,  $y=9.47273$ , and  $z=32.25$ . This gives a rough idea of the location of the tumor compared with the actual location of the tumor; therefore we can say that it can easily identify the tumor location. The real tumor location and the predicted tumor location can be seen in Fig. 14.

A comparison of several studies has been made in terms of antenna type, bandwidth, gain, and whether the study addresses cancer detection as intended. As seen in Table V [35-38], in terms of bandwidth, study [34] shows a better bandwidth, while better gain is presented by study [22]. While [35] and [36] have very efficient imaging, their design is more complicated, which increases

the (ROS) rate which is the risk of failure. Our study shows a better detection of cancer using the SAR analysis, with acceptable bandwidth and gain.

## VI. CONCLUSION

A  $60 \times 70$  mm microstrip circular patch antenna is designed for the detection of cancer at the early stages, with low cost and high efficiency. In the proposed design, copper is the conductive element used for the radiating surface, and for the defected ground with a circular microstrip patch, an FR-4 substrate has been used with  $\epsilon_r=4.3$ . Return loss analysis shows a bandwidth ranging from 1.6 GHz to 10 GHz under  $-10$  dB, and VSWR is below two for the entire band, which ensures good reflection efficiency. The breast phantom was created

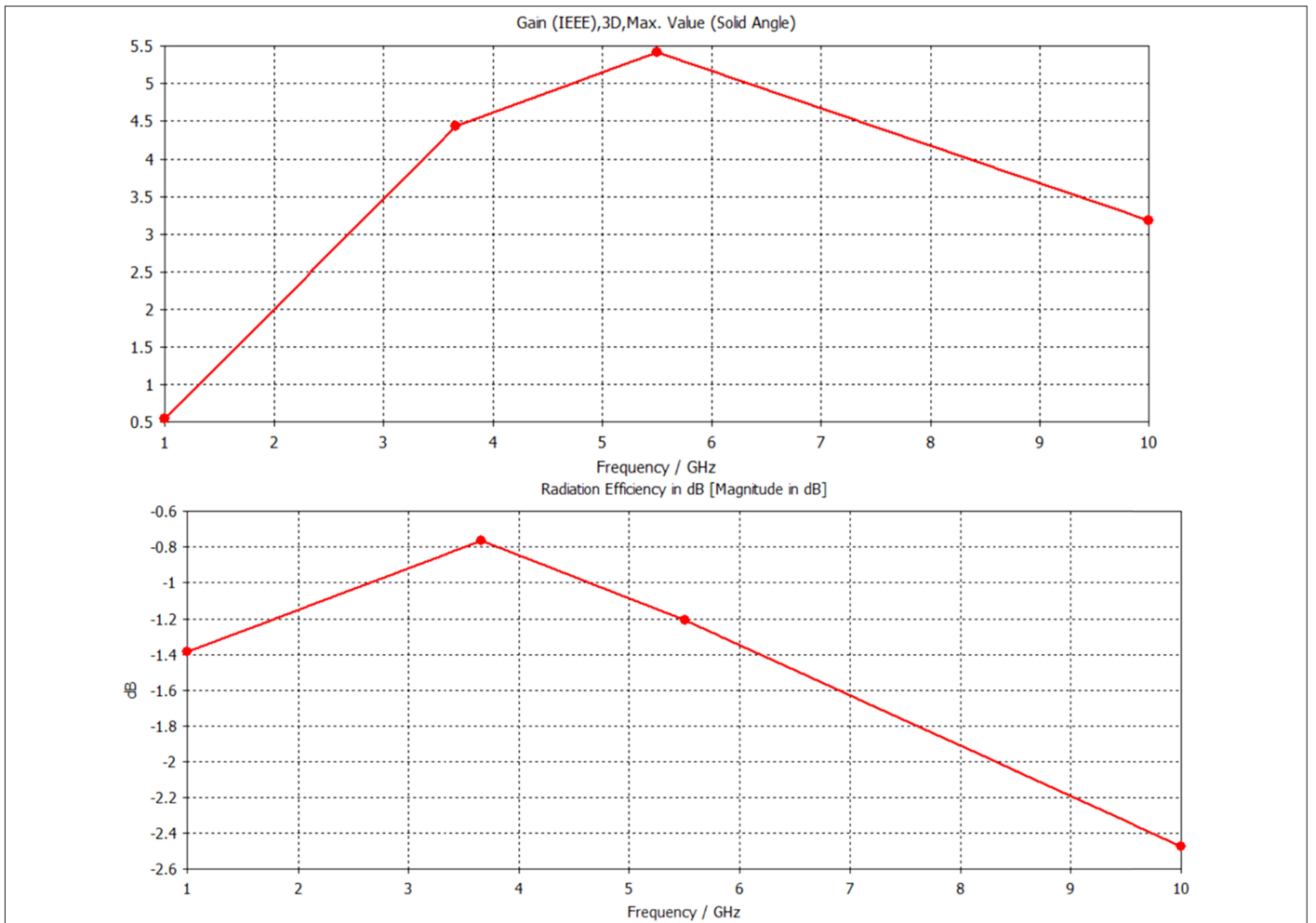


**Fig. 9.** Radiation gain and efficiency curves.

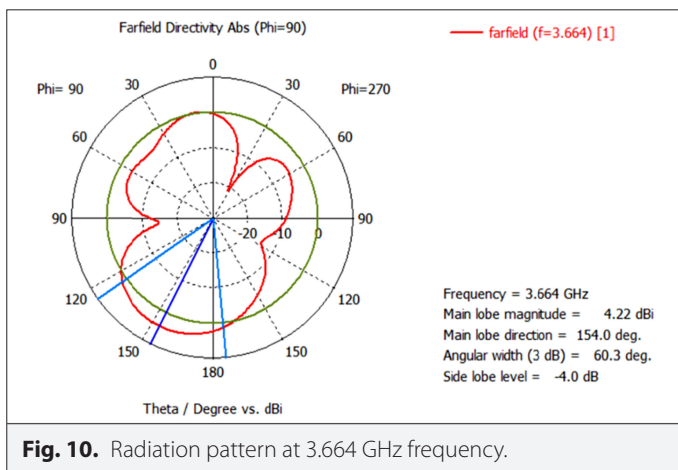


**Fig. 10.** Radiation pattern at 3.664 GHz frequency.

with a tumor located manually at (0, 10, 40) for the SAR analysis. The maximum SAR value is suitable for use in biomedical applications. The SAR maximum is at (1.085, 9.47273, 32.25), which indicates that the SAR value is higher at the location of the tumor cells, which enables the easy detection of cancer cells.

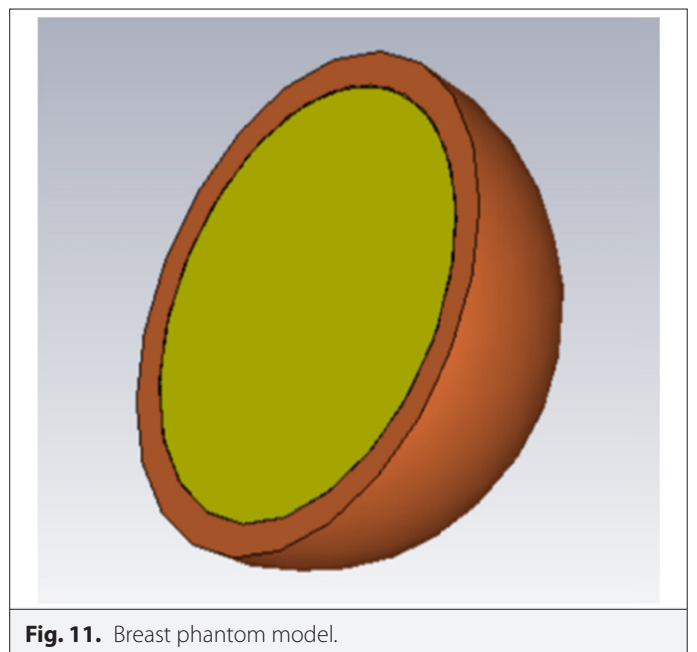


**Fig. 11.** Breast phantom model.

**TABLE III.** PARAMETERS OF THE BREAST PHANTOM

Tissue	Permittivity	Electrical Conductance	Density	Heat Capacity	Thermal Conductance
Skin	36.7	2.34	1109	3391	0.37
Fat	4.84	0.262	911	2348	0.21
Tumor	54.9	4	1058	-	-

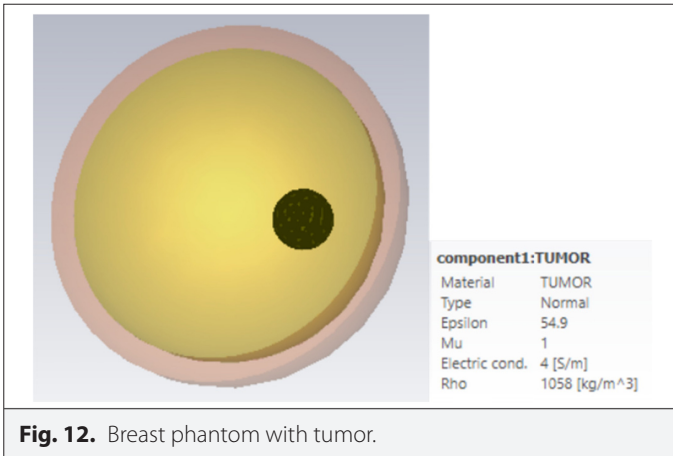


**Fig. 12.** Breast phantom with tumor.

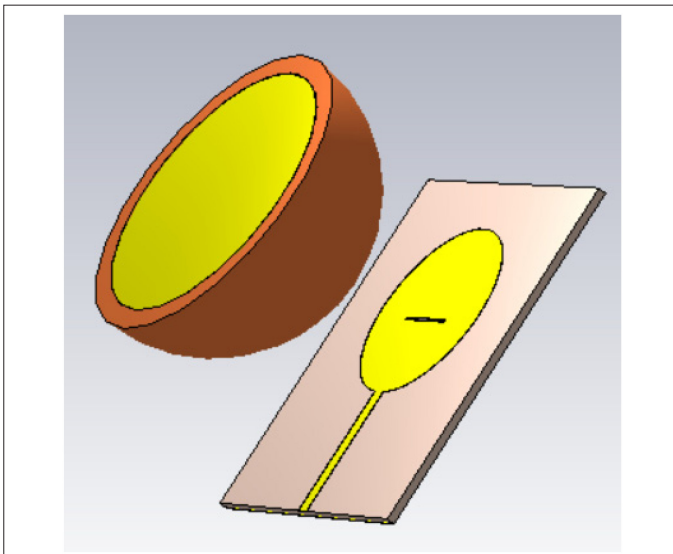


**Fig. 13.** Proposed antenna with breast phantom.

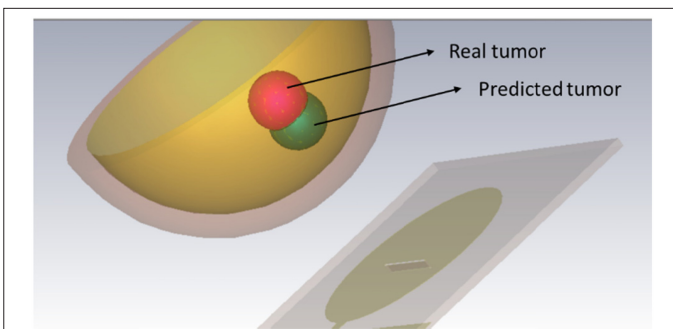


**Fig. 14.** SAR at 3.664 GHz.

**TABLE IV.** SAR RESULTS

SAR Calculation Results	
Power loss density monitor used	loss ( $f=3.664$ ) [1] at 3.664 GHz
Power scaling [W]	None
Stimulated Power [W]	0.5
Accepted Power [W]	0.499823
Average cell mass [g]	2.53793e-05
Averaging method	IEEE/IEC 62704-1
Averaging mass [g]	10
Entire Volume	
Min (x,y,z) [mm]	-45.1269, -49.6269, -13.7269
Max (x,y,z) [mm]	45.1269, 49.6269, 63.6269
Volume [mm <sup>3</sup> ]	692 939
Absorbed power [W]	0.07612
Tissue volume [mm <sup>3</sup> ]	56 547.9
Tissue mass [kg]	0.0555005
Tissue power [W]	0.0187236
Average power [W/mm <sup>3</sup> ]	3.3111e-07
Total SAR [W/kg]	0.337359
Max. point SAR [W/kg]	9.67361
Maximum SAR (10 g) [W/kg]	0.694738
Maximum at (x,y,z) [mm]	1.085, 9.47273, 32.25
Avg. vol. min (x,y,z) [mm]	-10.2492, -1.86151, 20.9158
Avg. vol. max (x,y,z) [mm]	12.4192, 20.807, 43.5842
Largest valid cube [mm]	22.7176
Smallest valid cube [mm]	21.9791
Avg. vol. accuracy [%]	0.0001
Calculation time [s]	38 457

**TABLE V.** COMPARISON TABLE BETWEEN OUR WORK AND OTHER WORK

Ref	Antenna Type	Bandwidth (GHz)	Gain (dBi)	Size (mm)	Cancer Detection
[34]	Metamaterial-Inspired Antenna Array	2–12	11	22 × 22	When several antennas are placed around a breast model, and when stimulated with EM radiation, the rings of sub-wavelength diameters behave as resonating components.
[35]	Antenna array of microstrip Vivaldi antenna	3.04–3.30	4.1	61 × 35	An antenna array was built having six microstrip Vivaldi antenna components.
[36]	MTM and SIW	600–622	≥1	1 × 1 × 0.1	N/A
[37]	Stair-shaped microstrip antenna	3.5–7.2	-	24 × 22	Based on Return Loss (High Error Rate)
[38]	Circular patch antenna	5.6–5.9	-	55 × 55	Based on Return Loss (High Error Rate)
This Work	UWB Circular Microstrip Antenna with SAR	1.6–10	4.431	60 × 70	SAR Analysis

**Peer-review:** Externally peer-reviewed.

**Author Contributions:** Concept – A.A.O., D.Ç.A.; Design – A.A.O.; Supervision – D.Ç.A.; Materials – A.A.O.; Data Collection and/or Processing – A.A.O.; Analysis and/or Interpretation – A.A.O., D.Ç.A.; Literature Search – A.A.O., D.Ç.A.; Writing Manuscript – A.A.O., D.Ç.A.; Critical Review – D.Ç.A.

**Conflict of Interest:** The authors have no conflicts of interest to declare.

**Financial Disclosure:** The authors declared that this study has received no financial support.

## REFERENCES

1. Y. Kuwahara, K. Suzuki, H. Horie, and H. Hatano, "Conformal array antenna with the aspirator for the microwave mammography," in *IEEE Antennas Propag. Soc. Int. Symp.*, 2010, pp. 10–13. [\[CrossRef\]](#)
2. F. F. Ting, K. S. Sim, and Y. Lee, "Three-dimensional model reconstruction using surface interpolation with the interfacing of Hermite surface for breast cancer MRI imaging system," in *Int. Conf. Robot. Autom. Sci. (ICORAS)*, 2016, pp. 1–5. [\[CrossRef\]](#)
3. C. Keatmanee, S. S. Makhanov, K. Kotani, W. Lohitvisate, and S. S. Thongvigitmanee, "Automatic initialization for active contour model in breast cancer detection utilizing conventional ultrasound and Color Doppler," in *Annu. Int. Conf. IEEE Eng. Med. Biol. Soc.*, 2017, pp. 3248–3251. [\[CrossRef\]](#)
4. C. A. Balanis, *Antenna Theory Analysis and Design*, 3rd ed. Hoboken, NJ, USA: Wiley, 2005.
5. K. Nahalingam and S. K. Sharma, "An investigation on microwave breast cancer detection by ultra-widebandwidth (UWB) microstrip slot antennas," in *IEEE Int. Symp. Antennas Propag. (APSURSI)*, 2011, vol. 1, pp. 3385–3388. [\[CrossRef\]](#)
6. R. M. Shubair and H. Elayan, "In vivo wireless body communications: State-of-the-art and future directions," in *Loughborough Antennas Propag. Conf. (LAPC)*, 2015, pp. 1–5. [\[CrossRef\]](#)
7. H. Elayan, R. M. Shubair, J. M. Jornet, and P. Johari, "Terahertz channel model and link budget analysis for intrabody nanoscale communication," *IEEE Trans. Nanobiosci.*, vol. 16, no. 6, pp. 491–503, 2017.
8. X. Li, E. J. Bond, B. D. Van Veen, and S. C. Hagness, "An overview of ultra-wideband microwave imaging via space-time beamforming for early-stage breast-cancer detection," *IEEE Antennas Propag. Mag.*, vol. 47, no. 1, pp. 19–34, 2005. [\[CrossRef\]](#)
9. M. M. Shirkolaee, "Wideband linear microstrip array antenna with high efficiency and low side lobe level," *Int. J. RF Microw. Comput. Aid. Eng.*, vol. 30, no. 11. [\[CrossRef\]](#)
10. M. Alibakhshikenari, B. S. Virdee, and E. Limiti, "Wideband planar array antenna based on SCRLH-TL for airborne synthetic aperture radar application," *J. Electromagn. Waves Appl.*, vol. 32, no. 12, pp. 1586–1599, 2018. [\[CrossRef\]](#)
11. A. A. Althuwayb, "Enhanced radiation gain and efficiency of a metamaterial-inspired wideband microstrip antenna using substrate integrated waveguide technology for sub-6 GHz wireless communication systems," *Microw. Opt. Technol. Lett.*, vol. 63, no. 7, pp. 1892–1898, 2021. [\[CrossRef\]](#)
12. M. Alibakhshikenari et al., "A comprehensive survey of "metamaterial transmission-line based antennas: Design, challenges, and applications," *IEEE Access*, vol. 8, pp. 144778–144808, 2020. [\[CrossRef\]](#)
13. M. Alibakhshikenari, B. S. Virdee, C. H. See, R. A. Abd-Alhameed, F. Falcone, and E. Limiti, "Super-wide impedance bandwidth planar antenna for microwave and millimeter-wave applications," *Sensors*, vol. 19, no. 10, p. 2306, 2019.
14. M. Alibakhshikenari, F. Babaeian, B. S. Virdee, S. Aissa, L. Azpilicueta, C. H. See, A. A. Athuwayb, I. Huynen, R. A. Abd-Alhameed, F. Falcone, and E. Limiti, "A comprehensive survey on various decoupling mechanisms with focus on metamaterial and metasurface principles applicable to SAR and MIMO antenna systems," *IEEE Access*, vol. 8, pp. 192965–193004, 2020. [\[CrossRef\]](#)
15. M. Alibakhshikenari, B. S. Virdee, P. Shukla, C. H. See, R. A. Abd-Alhameed, F. Falcone, K. Quazzane, and E. Limiti, "Isolation enhancement of densely packed array antennas with periodic MTM-photonics bandgap for SAR and MIMO systems," *IET Microwaves Antennas Propag.*, vol. 14, no. 3, pp. 183–188, 2020. [\[CrossRef\]](#)
16. H. Elayan, R. M. Shubair, and A. Kiourti, "Wireless sensors for medical applications: Current status and future challenges," in *11th Eur. Conf. IEEE Antennas Propag. (EUCAP)*, 2017, pp. 2478–2482.
17. H. Elayan and R. M. Shubair, "On channel characterization in human body communication for medical monitoring systems," in *17th Int. Symp. IEEE Antenna Tech. Appl. Electromagn. (ANTEM)*, 2016, pp. 1–2.
18. H. Elayan, R. M. Shubair, A. Alomairi, and K. Yang, "In-vivo terahertz channel characterization for nano-communications in WBANs," in *IEEE Int. Symp. IEEE Antennas Propag. (APSURSI)*, 2016, pp. 979–980.
19. H. Elayan, R. M. Shubair, and J. M. Jornet, "Bio-electromagnetic THz propagation modeling for in-vivo wireless nanosensor networks," in *11th Eur. Conf. IEEE Antennas Propag. (EUCAP)*, 2017, pp. 426–430.
20. H. Elayan, C. Stefanini, R. M. Shubair, and J. M. Jornet, "End-to-end noise model for intra-body terahertz nanoscale communication," *IEEE Trans. Nanobioscience*, vol. 17, no. 4, pp. 464–473, 2018.
21. H. Elayan, P. Johari, R. M. Shubair, and J. M. Jornet, "Photothermal modeling and analysis of intrabody terahertz nanoscale communication," *IEEE Trans. Nanobiosci.*, vol. 16, no. 8, pp. 755–763, 2017.

22. H. Elayan, R. M. Shubair, J. M. Jornet, and R. Mittra, "Multi-layer intrabody terahertz wave propagation model for nanobiosensing applications," *Nano Commun. Netw.*, vol. 14, pp. 9–15, 2017.
23. H. Elayan, R. M. Shubair, and N. Almoosa, "In vivo communication in wireless body area networks," in *Information Innovation Technology in Smart Cities*. Berlin, Germany: Springer, 2018, pp. 273–287.
24. M. O. AlNabooda, R. M. Shubair, N. R. Rishani, and G. Aldabbagh, "Terahertz spectroscopy and imaging for the detection and identification of illicit drugs," in *Sensors - Networks Smart Emerg. Tech. (SENSET)*, 2017, pp. 1–4.
25. E. C. Fear, P. M. Meaney, and M. A. Stuchly, "Microwaves for breast cancer detection?," *IEEE Potentials*, vol. 22, no. 1, pp. 12–18, 2003.
26. F. Alsharif and C. Kurnaz, "Wearable microstrip patch ultra wide band antenna for breast cancer detection," in *41st Int. Conf. Telecommun. Signal Process. (TSP)*, Athens, 2018, pp. 1–5. [\[CrossRef\]](#)
27. M. A. Afridi, "Microstrip patch antenna – designing at 2.4 GHz frequency," *Biological and Chemical Research*, Science Signpost Publishing, vol. 2015, p. 128–132, 2015.
28. R. Garg, *Microstrip Antenna Design Handbook*. Boston, MA, USA: Artech House, 2011.
29. M. M. Khan, A. K. M. Monsurul Alam, and R. H. Ashique, "A comparative study of rectangular and circular microstrip Fed Patch Antenna at 2.45 GHz," *Int. J. Sci. Eng. Res.*, vol. 5, no. 10, pp. 1028–1032, 2014.
30. H. M. Lee and W. Choi, "Effect of partial ground plane removal on the radiation characteristics of a microstrip antenna," *Wirel. Eng. Technol.*, vol. 4, no. 1, pp. 5–12, 2013.
31. D. Guha, S. Biswas, and Y. M. M. Antar, "Defected ground structure for microstrip antennas," in *Microstrip and Printed Antennas: New Trends, Techniques and Applications*. Hoboken, NJ, USA: Wiley, 2010, ch. 12. [\[CrossRef\]](#)
32. M. Miyakawa, S. Takata, and K. Inotsume, "Development of non-uniform breast phantom and its microwave imaging for tumor detection by CP-MCT," in *Annu. Int. Conf. IEEE Eng. Med. Biol. Soc.*, Minneapolis, MN, USA, 2009, pp. 2723–2726. [\[CrossRef\]](#)
33. J. Michałowska-Samonek, A. Miaskowski, and A. Wac-Włodarczyk, "Numerical analysis of high frequency electromagnetic field distribution and specific absorption rate in realistic breast models," *Electrotech. Rev.*, vol. 88, no. 12b, pp. 97–99, 2012.
34. M. Alibakhshikenari, B. S. Virdee, P. Shukla, N. O. Parchin, L. Azpilicueta, C. H. See, R. A. Abd-Alhameed, F. Falcone, I. Huynen, T. A. Denidni, and E. Limiti, "Metamaterial-inspired antenna array for application in microwave breast imaging systems for tumor detection," *IEEE Access*, vol. 8, pp. 174667–174678, 2020. [\[CrossRef\]](#)
35. F. Tasnim, F. Jannat, S. Kibria, M. S. Alam, T. Ahsan, T. Alam, R. Azim, and M. T. Islam, "Electromagnetic performances analysis of a Microwave Imaging System(MIS) for breast tumor detection," *Int. Conf. Innov. Sci. Eng. Technol. (ICISSET)*, 2018, pp. 442–446. [\[CrossRef\]](#)
36. A. A. Althuwayb, "On-chip antenna design using the concepts of metamaterial and SIW principles applicable to terahertz integrated circuits operating over 0.6–0.622 THz," *Int. J. Antennas Propag.*, vol. 2020, no. 6653095, 2020. [\[CrossRef\]](#)
37. A. Dewiani, E. Amir, I. Palantei, S. Areni, and A. Achmad, "Movement effect on electrical properties of UWB microwave antenna during breast tumor diagnostic scanning," *IEEE Asia Pac. Conf. Wirel. Mob. (APWiMob)*, 2015, pp. 188–191. [\[CrossRef\]](#)
38. F. M. Eltigani, M. A. A. Yahya, and M. E. Osman, "Microwave imaging system for early detection of breast cancer," in *Int. Conf. Commun. Control Comput. Electron. Eng. (ICCCCEE)*, 2017, pp. 1–5. [\[CrossRef\]](#)



Adel Al-Omairi received his first Diploma in ELECTRONICS/MEDICAL EQUIPMENT in 2013 from the institute of Medical Technology Al-MANSOR and was employed as a MEDICAL EQUIPMENT TECHNICIAN at the Central Teaching Hospital of Pediatrics in 2014, while at the same time, he was pursuing his studies in other fields. He received his bachelor's degree in COMMUNICATION ENGINEERING in 2017 from the AL-MAMON University college. He worked in private tutoring for different fields of engineering. He had his training in GSM and GPRS, Computer Networks, IP routing and switching at Huawei Training Center at BAGHDAD University in 2016. His main fields of interest are electromagnetics, antenna design, and medical engineering. He is currently pursuing his master's degree in ELECTRICAL AND COMPUTER ENGINEERING at ALTINBAS University.



Doğu Çağdaş Atilla received his Ph.D. degree in Electrical and Electronics Engineering in 2017 from Istanbul University and was employed as an instructor in the Electrical and Electronics Engineering Department. He worked on a number of Scientific Research Projects in Istanbul University between 2009 and 2018. He also worked as a full-time teaching assistant in Isik University between 2012 and 2017. His main fields of interest are electromagnetics, wide-band circuit design, antennas, and electric-autonomous vehicles. He currently holds five patents and has been employed as an assistant professor at Altinbas University from 2017. He is the academic advisor of the award winning project EVA Team (Electrical Vehicle of Altinbas) in the international efficiency car challenge of Turkey, and the project director of the TUAV Team challenging in UAV competitions. Besides, he serves as vice director of the Electric, Autonomous and Unmanned Vehicles Application and Research Center along with coordinatorship of the Institute of Graduate Studies.